



3-D Simulation of Particle and Gas Flow Behavior in a Riser with Venturi Pipe Inlet

Parinya Khongprom, Sunun Limtrakul*, Terdthai Vatanatham

Department of Chemical Engineering, Faculty of Engineering, Kasetsart University, Bangkok 10900, Thailand.

*Author for correspondence; e-mail: fengsui@ku.ac.th

Received : 17 October 2007

Accepted : 30 October 2007

ABSTRACT

The hydrodynamic behavior of a gas-solid flow in a 14-m high riser with a 45° inclined standpipe using a venturi pipe inlet was predicted using a transient three-dimensional hydrodynamic model. The model based on the kinetic theory of a granular flow was constructed using commercial computational fluid dynamics (CFD) software. The hydrodynamic behaviors of the gas-solid flow in the risers with a conventional straight pipe inlet and with a venturi pipe inlet were compared. In addition, the effect of throat diameter of the venturi pipe was studied. The solid concentration over the cross-sectional area of the riser is asymmetric because of the asymmetry of the particle inlet. The simulation results showed that a riser with a venturi pipe inlet can improve the solid flow behavior in the region near the riser entering region. In the riser with a venturi inlet, the solid particles flow in the standpipe with less gas blocking and higher velocity than those in a riser with a conventional inlet. The throat diameter has significant effects on the flow pattern in the riser. The solid velocity increases as the throat diameter decreases. Therefore, a venturi pipe inlet with proper design can decrease the backward gas flow into the standpipe.

Keywords: Riser, Simulation, Computational fluid dynamics, Hydrodynamics, Venturi pipe inlet.

1. INTRODUCTION

A circulating fluidized bed (CFB) is a highly effective reactor for gas-solid reaction systems. This reactor has been employed for a wide range of applications, including catalytic cracking, calcination, and combustion of a variety of fuels [1]. The bottom section of a CFB includes an inlet section of the riser and a returning system which is used for accommodating solid recirculation. The returning system of a CFB unit consists of a cyclone and standpipe. The standpipe is used for returning the solid back to the riser. The

outlet gas and solid particles from the riser are separated by the cyclone. The solid particles flow downward into the downer pipe and then are then fed into the riser through the standpipe. The geometry of a returning system has a significant effect on the flow behavior of gas and solid particles in the feed and return zones. Without a suitably designed riser, some riser-inlet gas might flow into the standpipe. In a riser with a conventional straight inlet, some riser gas also flows upward along the inclined standpipe

which is unavoidable. The slugging of gas can intermittently block the downflow of the particles in the standpipe. Therefore, a venturi inlet is proposed as a solid recirculation connector at the bottom inlet section of the riser. The venturi inlet consists of a narrow section (throat portion) where the pressure is low. This pressure drop enables gas and particles to be drawn into the riser.

There are many adjustable configurations and operating conditions for effective recirculation flow in the CFB. Construction and testing is tedious and time consuming work with a high cost. Therefore, simulations can be used to predict the behavior of systems with various geometries and operating conditions. In addition, the solids holdup and velocity profile in the system are important local information for design and operation. However, this local hydrodynamic information is rarely available in the literature. This is due to difficulty of experimental measurements.

In a gas-solid system with fine particles, the flow behavior of these particles has been described by the two-fluid model [2-5]. The flow behavior in a fluidized bed is usually predicted by the 2-D two-fluid model [6-7], which is suitable for a simple geometry such as a thin rectangular system or an axis-

symmetric cylindrical reactor. The bottom section of a CFB has a complex shape consisting of side pipes: hence the 2-D assumption is unacceptable and a 3-D simulation is required [8-9].

In this work, the simulation of flow behavior in riser with a 45° inclined standpipe was carried out to show the improvement of the solid flow entering the riser when using the venturi pipe inlet. A 3-D transient model based on the two-fluid model with the kinetic theory for the particle phase, was applied to predict the flow pattern in the standpipe and riser. The flow behaviors in risers with a venturi inlet and with a conventional straight inlet were compared. In addition, the effect of the venturi inlet size on the flow behavior was also studied. The local velocities and solids holdups in the riser zones were investigated.

2. MATHEMATICAL MODELING

The conservation equations of mass and momentum for the gas and solid phases are written in equations 1 to 3. For the solid phase, the transport equations for mass, momentum and granular temperature are obtained via the kinetic theory of a granular flow.

The continuity equation for phase i ($i =$ gas phase or solids phase) is written as

$$\frac{\partial}{\partial t}(\varepsilon_i \rho_i) + \nabla \cdot (\varepsilon_i \rho_i \vec{v}_i) = 0 \quad (1)$$

The conservation of momentum for the gas phase (g) yields

$$\frac{\partial}{\partial t}(\varepsilon_g \rho_g \vec{v}_g) + \nabla \cdot (\varepsilon_g \rho_g \vec{v}_g \vec{v}_g) = -\varepsilon_g \nabla p + \nabla \cdot \vec{\tau}_g + \varepsilon_g \rho_g \vec{g} + \beta(\vec{v}_s - \vec{v}_g) \quad (2)$$

The conservation of momentum for the solid phase (s) is

$$\frac{\partial}{\partial t}(\varepsilon_s \rho_s \vec{v}_s) + \nabla \cdot (\varepsilon_s \rho_s \vec{v}_s \vec{v}_s) = -\varepsilon_s \nabla p - \nabla p_s + \nabla \cdot \vec{\tau}_s + \varepsilon_s \rho_s \vec{g} + \beta(\vec{v}_g - \vec{v}_s) \quad (3)$$

The inter phase momentum transfer coefficient, β , can be written in the following form [10]:

$$\beta = \frac{3}{4} C_D \frac{\varepsilon_s \varepsilon_g \rho_g |\vec{v}_s - \vec{v}_g|}{d_s} \varepsilon_g^{-2.65} \quad (4)$$

where the drag coefficient is correlated as:

$$C_D = \frac{24}{\varepsilon_g \text{Re}_s} [1 + 0.15(\varepsilon_g \text{Re}_s)^{0.687}] \quad (5)$$

and the relative Reynolds number is defined as:

$$\text{Re}_s = \frac{\rho_g d_s |\vec{v}_s - \vec{v}_g|}{\mu_g} \quad (6)$$

The granular temperature for the solid phase is proportional to the kinetic energy of the random motion of the particles. The transport equation derived from the kinetic theory can be written in the form

$$\frac{3}{2} \left[\frac{\partial}{\partial t} (\rho_s \varepsilon_s \Theta_s) + \nabla \cdot (\rho_s \varepsilon_s \vec{v}_s \Theta_s) \right] = (-p_s \bar{I} + \bar{\tau}_s) : \nabla \vec{v}_s + \nabla \cdot (\kappa_{\Theta_s} \nabla \Theta_s) - \gamma_{\Theta_s} + \phi_{gs} \quad (7)$$

Constitutive equations are required to close the governing relation. These constitutive equations are summarized in Table I. The effects of turbulence are taken into account via the $k - \varepsilon$ turbulence model. The turbulence equations are shown in Table II.

Table I: Constitutive equations.

Solids pressure

$$p_s = \varepsilon_s \rho_s \Theta_s + 2 \rho_s (1 + e_{ss}) \varepsilon_s^2 g_{0,ss} \Theta_s$$

Radial distribution function

$$g_{0,ss} = \left[1 - \left(\frac{\varepsilon_s}{\varepsilon_{s,\max}} \right)^{\frac{1}{3}} \right]^{-1}$$

Solids shear viscosity

$$\mu_s = \mu_{s,col} + \mu_{s,kin} + \mu_{s,fr}$$

Solids collision viscosity

$$\mu_{s,col} = \frac{4}{5} \varepsilon_s \rho_s d_s g_{0,ss} (1 + e_{ss}) \left(\frac{\Theta_s}{\pi} \right)^{1/2}$$

Kinetic viscosity [11]

$$\mu_{s,kin} = \frac{\varepsilon_s d_s \rho_s \sqrt{\Theta_s \pi}}{6(3 - e_{ss})} \left[1 + \frac{2}{5} (1 + e_{ss})(3e_{ss} - 1) \varepsilon_s g_{0,ss} \right]$$

Solids frictional viscosity

$$\mu_{s,fr} = \frac{p_s \sin \phi}{2 \sqrt{I_{2D}}}$$

Solids bulk viscosity [12]

$$\lambda_s = \frac{4}{3} \varepsilon_s \rho_s d_s g_{0,ss} (1 + e_{ss}) \left(\frac{\Theta_s}{\pi} \right)^{1/2}$$

Diffusion coefficient of granular temperature [11]

$$\kappa_{\Theta_s} = \frac{15d_s \rho_s \varepsilon_s \sqrt{\Theta_s \pi}}{4(41 - 33\eta)} \left[1 + \frac{12}{5} \eta^2 (4\eta - 3) \varepsilon_s g_{0,ss} + \frac{16}{15\pi} (41 - 33\eta) \eta \varepsilon_s g_{0,ss} \right]$$

$$\eta = \frac{1}{2} (1 + e_{ss})$$

Collisional dissipation of energy [12]

$$\gamma_{\Theta_s} = \frac{12(1 - e_{ss}^2) g_{0,ss}}{d_s \sqrt{\pi}} \rho_s \varepsilon_s^2 \Theta_s^{3/2}$$

Transfer of the kinetic energy

$$\phi_{gs} = -3K_{gs} \Theta_s$$

Table II: $k - \varepsilon$ Turbulence model.

k -equation

$$\frac{\partial}{\partial t} (\rho_m k) + \nabla \cdot (\rho_m \vec{v}_m k) = \nabla \cdot \left(\frac{\boldsymbol{\mu}_{t,m}}{\sigma_k} \nabla k \right) + G_{k,m} - \rho_m \boldsymbol{\varepsilon}$$

ε -equation

$$\frac{\partial}{\partial t} (\rho_m \boldsymbol{\varepsilon}) + \nabla \cdot (\rho_m \vec{v}_m \boldsymbol{\varepsilon}) = \nabla \cdot \left(\frac{\boldsymbol{\mu}_{t,m}}{\sigma_\varepsilon} \nabla \boldsymbol{\varepsilon} \right) + \frac{\boldsymbol{\varepsilon}}{k} (C_{1\varepsilon} G_{k,m} - C_{2\varepsilon} \rho_m \boldsymbol{\varepsilon})$$

3. SIMULATION CONDITIONS

Figure 1 shows the riser and the returning systems used in this study. The riser reactor has 0.05 m diameter and 14.2 m height. Two types of bottom inlet sections of the riser were studied: conventional straight pipe inlet and venturi pipe inlet. The returning system consists of a particle inlet, storage tank, and hybrid angled standpipe. The standpipe is used for particle feeding into the riser. The angle between the standpipe and the riser is

45°. The throat diameters of the venturi pipes used in this study were 2.5, 3, and 4 cm. The throat length of the venturi pipe was equal to the riser diameter (D_r). The converging and diverging cone angles were 21° and 8°, respectively. At the tank inlet, the solid and gas velocities, and solid fraction were specified. However, the gas velocity was only specified for the riser inlet gas; which is assumed to be uniform across the riser sectional area. The simulations were carried out using the

computational fluid dynamics software package named Fluent version 6.2. Fluid catalytic cracking (FCC) particles and air were used as the solid and gas phases, respectively.

The physical properties of the particles and the simulation conditions are shown in Table III.

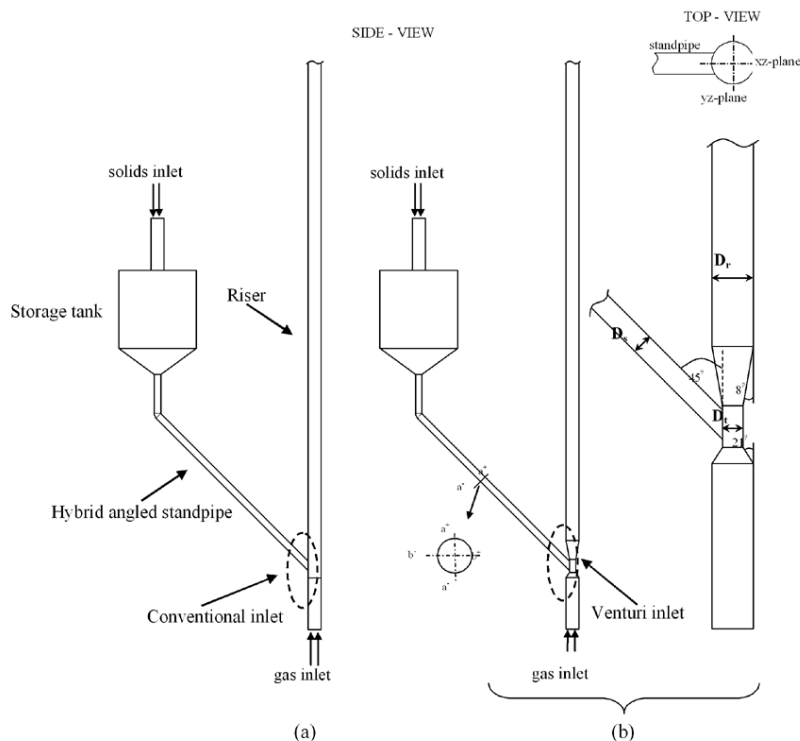


Figure 1. The geometry of riser reactor used for the simulation (a) with a conventional inlet (b) with a venturi inlet.

Table III: The physical properties of the particles and the simulation conditions.

Properties	Value
Particle diameter (um)	76
Particle density (kg/m ³)	1,712
Riser diameter (m)	0.05
Riser height (m)	14.2
Throat diameter (m)	0.025,0.03,0.04
Time step size (sec.)	1.0X10 ⁻⁵
Inlet conditions	Value
Tank solids inlet	solids velocity; 0.2 m/s gas velocity; 0.2 m/s solid fraction; 0.4
Riser gas inlet	10 m/s

4. RESULTS AND DISCUSSION

4.1 Flow behavior in the standpipe

Figure 2 shows the solid volume fraction and velocity vector profiles in the standpipe and riser. The solid concentration profiles show that the gas and solids are segregated in the standpipe, which were also observed in the experiments of Karri et al. and Sauer et al., [13, 14]. Most solid particles flow downward along with the downflow of gas from the tank into the lower portion of the standpipe cross section, while some gas from the riser inlet flows upward in the upper portion as shown in Figure 2 (b). Comparing the two types of riser, the riser with a venturi inlet has fewer gas bubbles flowing upward in the upper portion of the standpipe cross

section while the particles flow downward along the bottom section of the standpipe with less gas blocking. Figure 3 shows the time-averaged axial velocities of gas and particles in the middle section of the standpipe. The a-a and b-b lines are vertical and horizontal lines through the axis of the standpipe. It can be seen that the downflow gas and solid velocities in the standpipe for the system with a venturi inlet are higher than those in the system with a conventional inlet. From the venturi principle, the pressure in the throat portion decreases while the velocity increases. This pressure drop enables gas and solids to be drawn into the riser resulting in higher gas and solids velocities in the standpipe.

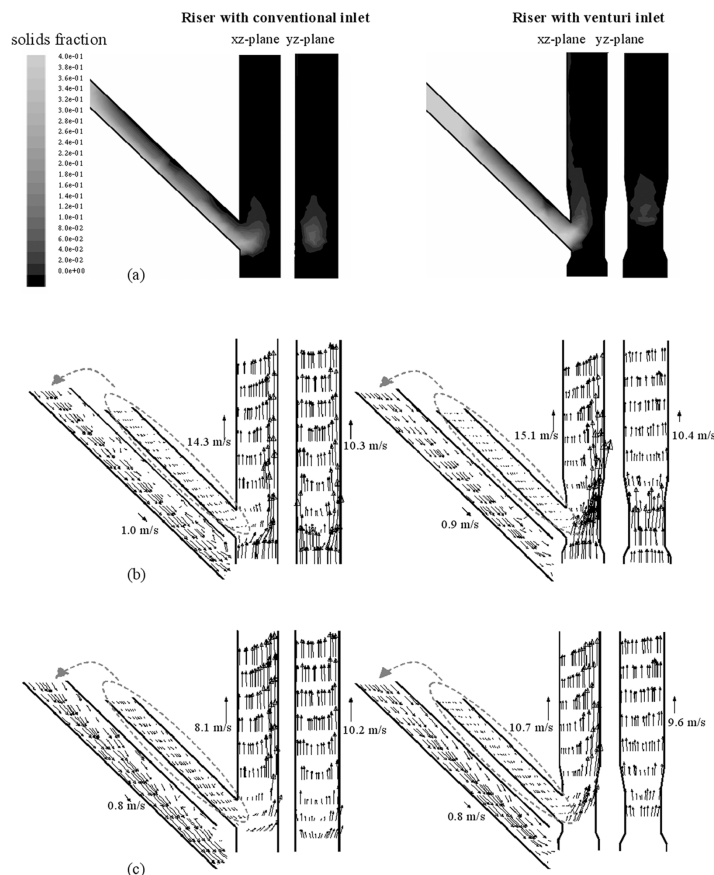


Figure 2. Solids volume fraction and velocity profiles in the standpipe and riser at 7 sec. (a) solids volume fraction (b) gas velocity vectors (c) solids velocity vectors.

4.2 Flow behavior in the inlet area of the riser

The solid concentration is high in the connecting area of standpipe and the riser, especially in the conventional riser. Figure 2 (b) shows that gas velocities in the riser junction area which is a dense zone are low and the riser gas velocity beside and opposite the particle inlet pipe is high. This higher velocity is the result of gas channeling away from the dense particle region. Thus the axial solid velocity profiles show off-center maxima (Figure 2 (c)). This behavior has also been reported by Van Engelandt et al., [15]. Figure

4 shows the time-averaged axial and radial solid velocities in the inlet zone of the riser. In a conventional riser, the comparison of the simulation and experimental results, as obtained by Van Engelandt et al. [15], shows that the axial solid velocities are low in the central region. However, the simulated solid velocities near the wall region are significantly lower than the experimental results (see Figure 4). Therefore, the wall boundary condition should be modified to obtain more accurate results. In a more realistic model, at the wall, a slip boundary condition can be applied for the solid phase. Then the simulated solids

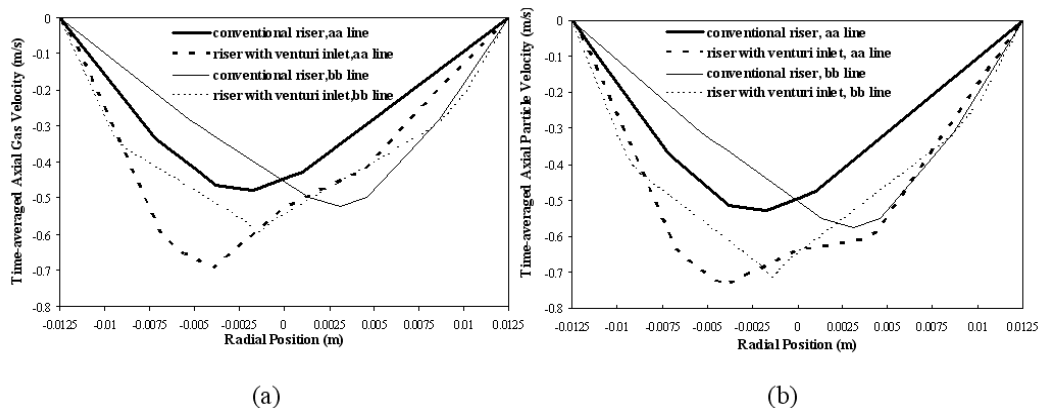


Figure 3. Time-averaged axial velocity in the middle section of the standpipe, throat diameter = 4 cm. (a) gas phase (b) solids phase.

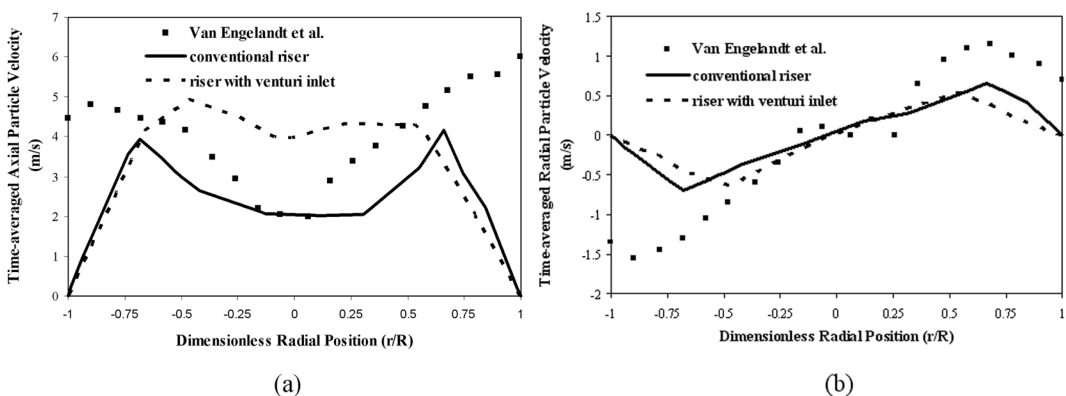


Figure 4. Time-averaged solids velocity in the inlet zone of the riser in the YZ plane along the Y-axis (radial direction), throat diameter = 4 cm. (a) time-averaged axial solids velocity (b) time-averaged radial solids velocity.

velocity should be better fitted to the experimental velocity. Comparing the velocities in the riser between a venturi inlet and the conventional riser, it was found that the axial solid velocity in the riser with a venturi inlet is higher, while the radial solid velocity is slightly lower (see Figure 4 (b)).

4.3 Effect of throat diameter

Figure 5 shows gas velocity vectors in risers with different throat diameters. In the

riser with a smaller throat diameter, gas velocity is higher in consistency with the mass conservation, especially at the opposite side of the solid feeding inlet. The high gas velocity leads to non-uniform flow above the connecting point of the standpipe and the riser (Figure 5 (c)). Figure 6 shows the time-averaged axial solid velocity profiles along the radial direction. The simulation results show that solid velocity increases slightly as the throat diameter decreases.

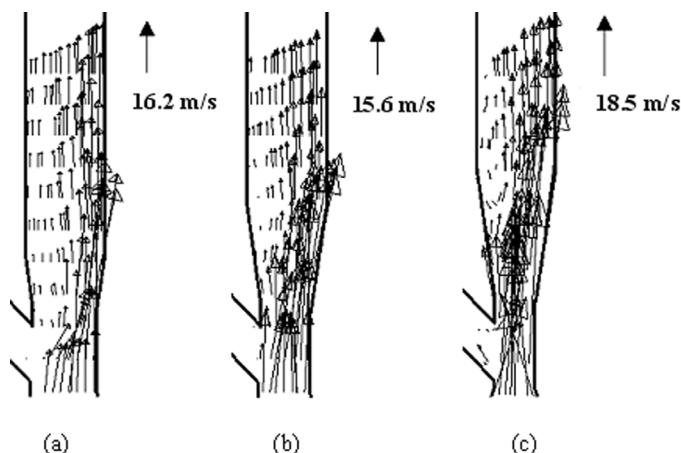


Figure 5. Gas velocity in the XZ plane at 7 sec., throat diameter (a) = 4 cm. (b) = 3 cm. (c) = 2.5 cm.

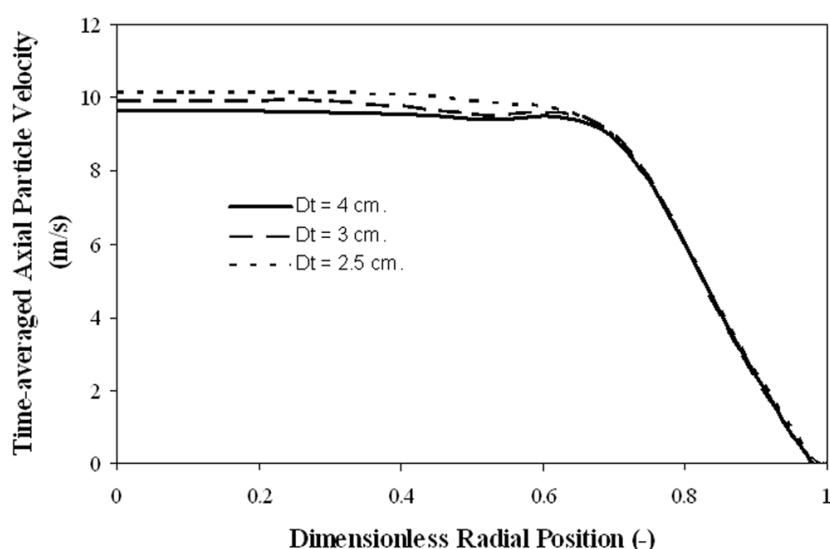


Figure 6. Time-averaged axial solids velocity in the riser with various venturi pipe inlet diameter (D_t) at $H = 1.2$ m.

5. CONCLUSIONS

The solid concentration distribution over the cross-sectional area of the riser is asymmetric because of the asymmetry of the solid inlet. The riser with a venturi pipe inlet can improve the flow of particles entering the bed. The solid particles flow in the standpipe with less gas blocking and higher velocity. The axial solids velocity in the riser with a venturi pipe inlet is higher than that of the conventional riser. In addition, the axial solid velocity profiles show off-center maxima. In the venturi pipe inlet, the gas velocity increases through the throat section due to the decreasing pressure. Therefore gas and particles are sucked into the riser with higher velocities because of the pressure drop inside the throat. The venturi pipe inlet with proper design can decrease the backward gas flow into the standpipe. Moreover, the solid velocity increases slightly as the throat diameter of the venturi pipe decreases.

ACKNOWLEDGEMENTS

This work was financially supported by the Thailand Research Fund (TRF) under the Research Career Development Project and the Royal Golden Jubilee Ph.D. Program, and Kasetsart University Research and Development Institute (KURDI).

REFERENCES

- [1] Grace J.R., Avidan A.A., and Knowlton T.M., *Circulating Fluidized Beds*, 1st Edn., Blackie Academic & Professional, London, 1997.
- [2] Arastoopour H., Numerical Simulation and Experimental Analysis of Gas/Solid Flow Systems, *Powder Technol.*, 2001; **119**: 59–67.
- [3] Jiradilok V., Gidaspow D., Damronglerd S., Koves W.J., and Mostofi R., Kinetic Theory Based CFD Simulations of Turbulent Fluidization of FCC Particles in a Riser, *Chem. Eng. Sci.*, 2006; **61**: 5544–5559.
- [4] Luben C.G., and Femando E.M., Collisional Solid's Pressure Impact on Numerical Results from a Traditional Two-Fluid Model, *Powder Technol.*, 2005; **149**: 78–83.
- [5] Zheng Y., Wan X., Qian Z., Wie F., and Jin Y., Numerical Simulation of the Gas-Particle Turbulent Flow in Riser Reactor Based on $k - \varepsilon - k_p - \varepsilon_p - \Theta$ Two-Fluid Model, *Chem. Eng. Sci.*, 2001; **56**: 6813–6822.
- [6] Benyahia S., Arastoopour H., Knowlton T.M., and Massah H., Simulation of Particles and Gas Flow Behavior in the Riser Section of a Circulating Fluidized Bed Using the Kinetic Theory Approach for the Particulate Phase, *Powder Technol.*, 2000; **112**: 24–33.
- [7] Huilin L., Gidaspow D., Bouillard J., and Wentie L., Hydrodynamic Simulation of Gas–Solid Flow in a Riser Using Kinetic Theory of Granular Flow, *Chem. Eng. J.*, 2003; **95**: 1–13.
- [8] Almuttahar A., and Taghipour F., Computational Fluid Dynamics of High Density Circulating Fluidized Bed Riser: Study of Modeling Parameters, *Powder Technol.*, In press.
- [9] Benyahia S., Arastoopour H., and Knowlton T.M., Two-dimensional Transient Numerical Simulation of Solids and Gas Flow in the Riser Section of a Circulating Fluidized Bed, *Chem. Eng. Comm.*, 2002; **189**: 510–527.
- [10] Wen C.Y., and Yu Y.H., Mechanics of Fluidization, *Chem. Eng. Prog. Symp.*, 1966; **62**: 100–111.
- [11] Syamlal M., Rogers W., and O'Brien T. J., *MFIX Documentation: Volume 1, Theory Guide*. National Technical Information Service, Springfield, 1993.

- [12] Lun C.K.K., Savage S.B., Jeffrey D.J., and Chepurniy N., Kinetic Theories for Granular Flow: Inelastic Particles in Couette Flow and Slightly Inelastic Particles in a General Flow Field, *J. Fluid Mech.*, 1984; 140: 223-256.
- [13] Karri S.B.R., and Knowlton T.M., Comparison of Group A Solids Flow in Hybrid Angled and Vertical Standpipes in: 4th Circulating Fluidized Bed Technology (ed. A. Avidan), AIChE, New York, 1993; 253-259.
- [14] Sauer R.A., Chan I.H., and Knowlton T.M., The Effects of System and Geometrical parameters on the flow of Class-B Solids in Overflow Standpipes, AIChE Symposium Series, 1984; 234: 1.
- [15] Van Engelandt G., Wilde J.D., Heynderickx G.J., and Marin G.B., Experimental Study of Inlet Phenomena of 35° Inclined Non-aerated and Aerated Y-inlets in a Dilute Cold-flow Riser, *Chem. Eng. Sci.*, 2007; 62: 339-355.